Automated Two-stage Conversion of Hourly Optimal DC Flow Solution to AC Power Flow

Adedasola A. Ademola, *Student Member*, *IEEE*, Shutang You, *Member*, *IEEE*, and Yilu Liu, *Fellow*, *IEEE*

***Abstract*—Conversion of hourly dispatch cases derived using DC optimal power flow (DCOPF) to AC power flow (ACPF) case is often challenging and requires arduous human analysis and intervention. This paper proposes an automated two-stage approach to solve ACPF formulated from DCOPF dispatch cases. The first stage involved the use of the conventional Newton Raphson method to solve the ACPF from flat start, then ACPF cases that are unsolvable in the first stage are subjected to a hot-starting incremental method, based on homotopy continuation, in the second stage. Critical tasks such as the addition of reactive power compensation and tuning of voltage setpoints that typically require human intervention were automated using a criteria-based selection method and optimal power flow respectively. Two datasets with hourly dispatches for the 243-bus reduced WECC system were used to test the proposed method. The algorithm was able to convert 100% of the first set of dispatch cases to solved ACPF cases. In the second dataset with suspect dispatch cases to represent an extreme conversion scenario, the algorithm created solved ACPF cases that satisfied a defined success criterion for 77.8% of the dispatch cases. The average run time for the hot-starting algorithm to create a solved ACPF case for a dispatch was less than 1 minute for the reduced WECC system.**

***Index Terms*—AC power flow, DC power flow, hot-starting algorithm, homotopy continuation, power flow convergence, reactive power compensation, voltage setpoint tuning.**

I. Introduction

With the growing penetration of variable renewable energy generators in power grids, system planners are increasingly interested in performing stability assessments of the grid under numerous future scenarios [1], [2]. Snapshots of the power grid under these future scenarios are often required for these studies. The creation of these snapshots usually involves production cost modeling (PCM) which considers forecasted load, generator production costs and constraints, fuel costs, transmission constraints, emission constraints, and even market competition, to provide the security-constrained economic dispatch of grid generators to meet loading. Ideally, PCM will use full AC optimal power flow (ACOPF) as the basis to combine market and physics parameters in its calculations. However, ACOPF solution is extremely computationally expensive for practical power systems due to nonconvexities and multipart nonlinear pricing [3]. Therefore, the more robust and faster DC optimal power flow (DCOPF) is widely used to calculate the least-cost hourly or sub-hourly generation dispatch in response to forecasted load demand. DCOPF is not to be confused as a power flow solution for a direct current network, rather, it is a version of ACOPF simplified by assuming that voltage magnitudes are fixed, voltage angles are close to zero, and in many cases, transmission losses are negligible [3]. Since DCOPF is based on DC power flow (DCPF), the created dispatch cases only include active power generation and load demand usually without consideration for system parameters like line losses, reactive power flow, and bus voltage profiles. These system parameters are vital to performing stability studies e.g., voltage stability studies. Thus, the conversion of the DCOPF dispatch case to a full AC power flow (ACPF) case is often required for further stability studies.

Traditionally, only a few snapshot dispatch cases are converted to ACPF e.g., summer peak case and spring light case. However, these snapshot cases are becoming insufficient to inform grid planners in the modern power systems due to increase in sub-hourly transactions among balancing authorities and higher penetration of intermittent renewable generation. It is therefore increasingly necessary to convert many hourly (or sub-hourly) dispatch cases to equivalent ACPF cases. This conversion process can be challenging, being described as 'maddening difficult' in [3], especially because DCOPF dispatch solutions are hardly ever AC-feasible [4]. The conversion often requires heuristic parameter tuning and manual voltage support addition to make the DCOPF dispatch cases solvable in ACPF. But such manual conversion is impractical for a large number of dispatch cases, e.g., for all 8,760 hours in a year, especially for systems with hundreds or thousands of buses [5]. It is therefore surprising that no commercial software vendor is offering a tool to automate this conversion process. Hence, this paper presents a two-stage process to serve as a blueprint for the automated conversion of a large number of dispatch cases to solved ACPF cases.

Equations (1) and (2) represent the ACPF mathematical formulation.

Manuscript received November 28, 2021; revised March 16, 2022; accepted May 12, 2022. Date of online publication August 18, 2022; date of current version September 26, 2022. This work was supported by the ERC Program of the National Science Foundation and DOE under NSF Award Number EEC-1041877, the CURENT Industry Partnership Program, and the Bredesen Centre, University of Tennessee, Knoxville.

A. A. Ademola (corresponding author, e-mail: aademol1@vols.utk.edu) is with the Bredesen Centre, and Centre of Ultra-Wide Area Resilient Electrical Energy Transmission Networks, University of Tennessee, Knoxville, TN 37996 USA.

S. You is with Centre of Ultra-Wide Area Resilient Electrical Energy Transmission Networks, University of Tennessee, Knoxville, TN 37996 USA.

Y. Liu is with Centre of Ultra-Wide Area Resilient Electrical Energy Transmission Networks, University of Tennessee, Knoxville, TN 37996 USA. and Oak Ridge National Laboratory, Knoxville, TN 37830 USA.

DOI: 10.17775/CSEEJPES.2021.08870

$$P_i^{\text{inj}} = V_i \sum_{j=1}^{N_{\text{bus}}} V_j \left(g_{ij} \cos\left(\theta_i - \theta_j\right) + b_{ij} \sin\left(\theta_i - \theta_j\right)\right) \quad (1)$$

$$Q_i^{\text{inj}} = V_i \sum_{j=1}^{N_{\text{bus}}} V_j \left(g_{ij} \sin\left(\theta_i - \theta_j\right) - b_{ij} \cos\left(\theta_i - \theta_j\right)\right)$$
$$i, j = 1, \ldots, N_{\text{bus}} \quad (2)$$

where P_i^{inj} and Q_i^{inj} are active and reactive power injections at bus i, respectively; V and θ are bus voltage magnitudes and angles respectively; g and b are branch conductance and susceptance respectively; N_{bus} is the number of buses in the network.

Equations (1) and (2) are usually solved by variations of the Newton Raphson (N-R) method [4], which may fail to converge to a solution [5], or may converge to undesirable low voltage solutions [6]. The N-R method was developed based on the assumption that higher-order terms of Taylor's series expansion of a non-linear function can be neglected. This is only true if the initial solution guess is sufficiently close to the final solution and within its domain of attraction [7]. Thus, ACPF solution using the N-R method is notoriously sensitive to initial voltage guesses and the generic flat-start guesses ($1\angle 0$ p.u. voltage at all buses) have been reported to rarely work for real systems [8], [9]. To make better-than-flat-start initial voltage guesses, [10] and [11] proposed the use of approximate solutions from linearized power flow models such as DCPF to provide a better starting point for the N-R method. However, this approach is unsuitable for ill-conditioned or heavily loaded systems for which linearized power flow models often provide low accuracy or unreasonable solutions [12]. Artificial intelligence techniques such as machine learning and deep learning have also been proposed to provide initial voltage guesses, but this approach requires sufficient and representative training data which may not be readily available [13]–[15]. Ref. [16] and [17] deployed homotopy continuation to provide good initialization for a difficult ACPF case by replacing it with a sequence of subcases where the first subcase is a suitable base case with known solutions, and the last subcase corresponds to the target ACPF to be solved. While useful, the choice of a suitable base case is not trivial and there are no established criteria for its choice.

Even with good initializations, an ACPF at certain operating points may have no solution [6], [7]. Studies in [18]–[21] focused on finding the minimum load shedding required to restore solvability of the power flow. These methods are unsuitable for ACPF with invariable load dispatch fixed by external considerations such as load forecast. Reactive power (MVar) compensation can be used to increase the region of solvability (RS) of ACPF while maintaining load [22]–[24]. However, appropriate sizing and location of the MVar compensation devices can be challenging, especially when autonomous placements are desired.

The main contribution of this paper is the conversion of a large number of hourly dispatches from DCOPF to solved ACPF cases using a hot-starting incremental algorithm. The algorithm combines homotopy continuation and MVar compensation methods to improve the robustness of the N-R method against bad initializations and expand the RS of ACPF at difficult operating points respectively. While previous methods have focused on reducing load to solve the ACPF [21], the proposed work uses MVar compensation to improve power transfer capability and expand the RS to solve ACPF without changing load dispatch. To eliminate human intervention in the conversion process, fully automatable methods were deployed to identify appropriate locations to connect MVar compensators and tune the voltage setpoints for regulated buses.

The rest of the paper is organized as follows. Section III introduces the two stages of the proposed DCPF to ACPF conversion process. In Section IV, two sets of hourly dispatch cases for the reduced Western Electricity Coordinating Council (WECC) system were used to show the performance of the conversion process. Section V concludes the paper and highlights potential areas of future research.

II. Conversion of Hourly Dispatch Cases From DCOPF to Solved ACPF

The conversion process involves two stages. The first stage is a simple DC-to-ACPF conversion using the N-R method to solve created ACPF cases. The voltage magnitudes and angles are initialized from flat start. The hourly ACPF cases that are not solvable in the first stage are passed on to the second stage where the hot-starting incremental algorithm is used to solve them. An ACPF is considered solved if the largest power mismatch at any bus is not greater than 0.1 MW (or MVAr) and voltage at a regulated bus, not at its maximum reactive power limit, is within ± 0.001 p.u. of its voltage setpoint. Fig. 1 is a block diagram showing the inputs and outputs of each stage of the conversion process and the following sub-sections explain each stage.

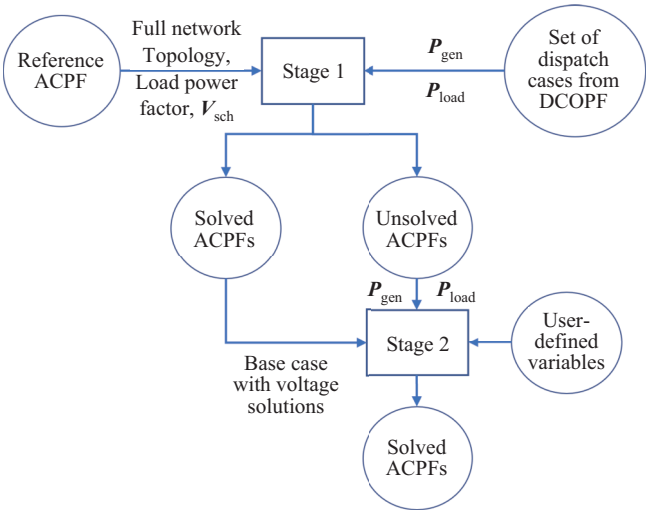

Fig. 1. Inputs and outputs of the DCPF to ACPF conversion stages.

A. Stage 1: Simple DC-to-ACPF Conversion

The simple DC-to-ACPF conversion made use of a reference ACPF case already formulated and solved in PSS/E, with full network topology information, voltage setpoints for regulated buses, $\boldsymbol{V}_{\text{sch}}$, and load power factors. The topology in the

DCOPF solver should be the same as that of the reference case. To create an equivalent ACPF for each hourly dispatch case, the active power generation, $\boldsymbol{P}_{\text{gen}}$, and the active load demand, $\boldsymbol{P}_{\text{load}}$, of the reference ACPF are replaced by the $\boldsymbol{P}_{\text{gen}}$ and $\boldsymbol{P}_{\text{load}}$ of the hour. Reactive load demand, $\boldsymbol{Q}_{\text{load}}$, is calculated using the load power factors for each bus in the reference ACPF. At this stage, the known parameters, $\boldsymbol{P}_{\text{gen}}$, $\boldsymbol{P}_{\text{load}}$, $\boldsymbol{Q}_{\text{load}}$, and $\boldsymbol{V}_{\text{sch}}$, are sufficient to formulate the power flow mismatch equations (1) and (2). Thus, the N-R method is used to calculate the final voltage magnitudes, $\boldsymbol{V}$, and angles, δ, at all buses, as well as the reactive power generation, $\boldsymbol{Q}_{\text{gen}}$, at all generators. Fig. 2 presents the algorithm of the simple DC-to-ACPF conversion.

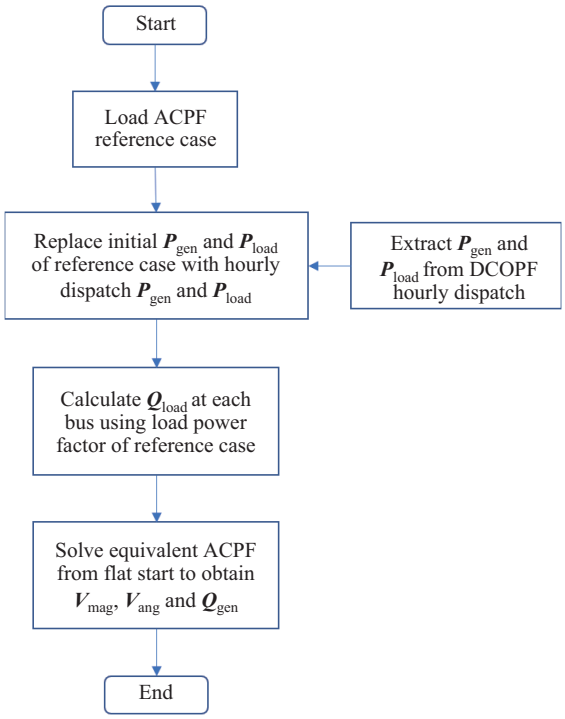

Fig. 2. Simple DC-to-ACPF conversion algorithm.

B. Stage 2: Hot-starting Incremental Algorithm

This stage involves the deployment of a hot-starting incremental algorithm that borrows the general idea of the homotopy-continuation method. For this work, the chosen homotopy parameters are $\boldsymbol{P}_{\text{gen}}$, $\boldsymbol{P}_{\text{load}}$, $\boldsymbol{Q}_{\text{gen}}$. Suitable solved cases from stage 1 are used as starting base cases for the hot-starting algorithm. To facilitate solution, the algorithm also incorporates automated MVar compensation using a criteria-based selection method and tuning of voltage setpoints was achieved using optimal power flow (OPF). The block diagram in Fig. 3 presents the workflow of the hot-starting algorithm, and the following sub-sections delineate each block.

1) Identification of Suitable Starting Base Case

In practice, it was found that hot-starting a solution from a base case with highly disparate generator dispatch impacts the chances and speed of getting an ACPF solution at the target dispatch. If the ACPF cases are available in time sequence, e.g., for each hour of a year, an obvious solution will be to use solved ACPF cases close in time-period to the target ACPF as a base case. However, this is sub-optimal in the presence of variable renewable energy generators which sometimes introduce large differences in dispatch between cases close to each other in time. Thus, a more systematic approach was developed to identify the most suitable starting base case among candidate solved cases using two criteria presented as follows.

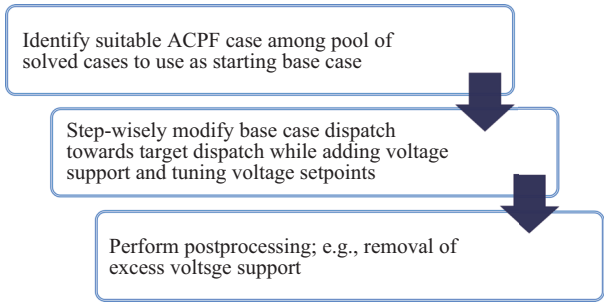

Fig. 3. Workflow of the developed hot-starting incremental algorithm.

a) Unit Commitment Similarity Score (UCSS): The UCSS relates the operational generator units in a candidate solved case to that of the target case to be solved. It is given as:

$$\begin{aligned} \text{UCSS}_{\text{c}} &= \sum_{i=1}^{N_{\text{gen}}} \overline{u_{i,\text{t}} \oplus u_{i,\text{c}}} \\ u_i &= 1 \qquad \text{if } P_i > 0 \\ &= 0 \qquad \text{otherwise} \end{aligned} \tag{3}$$

where N_{gen} is the number of generators; P_i is the active power of generator i; t indicates target case; c indicates candidate case; $\overline{\oplus}$ is the EX-NOR logic operator.

The candidate case with the highest UCSS is chosen as the starting base case. When there is a tie, the next criterion is used.

b) Mean-squared Difference (MSD): To choose among candidate cases with the same UCSS, the mean squared difference between the generator dispatch of each candidate case and the target case is calculated using (4). All variables are the same as in (3).

$$\text{MSD}_{\text{c}} = \frac{1}{N_{\text{gen}}} \sum_{i=1}^{N_{\text{gen}}} (P_{i,\text{t}} - P_{i,\text{c}})^2 \tag{4}$$

Among candidate cases with the same UCSS, the one with the least MSD relative to the target case is chosen as the starting base case.

2) Stepwise Modification of Base Dispatch Towards Target Dispatch

After identifying and loading a suitable starting base case, the hot-starting algorithm adjusts the initial dispatch (i.e., $\boldsymbol{P}_{\text{gen,c}}$, $\boldsymbol{P}_{\text{load,c}}$, and $\boldsymbol{Q}_{\text{load,c}}$) towards the target dispatch (i.e., $\boldsymbol{P}_{\text{gen,t}}$, $\boldsymbol{P}_{\text{load,t}}$, and $\boldsymbol{Q}_{\text{load,t}}$) to indirectly solve the target ACPF case. Before the adjustment process, participating generators in the target ACPF case that are shut down in the starting base case are turned on. During the dispatch

adjustment process, the following are the salient decisions the algorithm is programmed to make.

a) Step Size: The algorithm calculates the appropriate step size to use for each conversion process. Larger step sizes from initial dispatch to target dispatch will improve speed but tend to create unstable or divergent ACPF cases. On the other hand, smaller step sizes will lead to slower run time. Thus, a balance between speed and stability was established by calculating the step sizes as a function of the maximum difference in generator dispatch between a base case and the target case, as given below:

$$s_i = \frac{P_{\mathrm{t},i} - P_{\mathrm{b},i}}{f \times \max(|P_{\mathrm{t},i} - P_{\mathrm{b},i}|)} \tag{5}$$

where s_i is the step-size at generator i; $P_{\mathrm{t},i}$ and $P_{\mathrm{b},i}$ are the real power at generator i for target and base case, b, respectively (excluding slack generators); f is a variable factor.

The addition of the variable, f, in (5) allows the algorithm to vary the step-size such that initial f (or f_{init}) is small at the start to make step sizes large when dispatch is still close to the base case and the ACPF is still more stable. Then, f is gradually increased by Δf to lower the step size as dispatch is brought closer to the target case when the ACPF is usually more fragile. A maximum f value, $f_{\max}$, should be set to signal the smallest step size that the algorithm is allowed to take before it must stop.

b) Identification of Buses in Need of Voltage Support: Voltage support using switched shunt devices with high reactive power and continuous voltage control are added to buses that fall into these two categories:

1) Buses with voltage less than 0.9 p.u.
2) Buses with the highest voltage instability per N-R iteration for a repeatedly unconverging ACPF.

These buses are identified any time a base case is loaded before dispatch adjustment begins. For the first category, shunt devices are only added to violating bus with the least voltage until all bus voltages rise above 0.9 p.u. This is because voltage support at one bus will affect other buses within its sphere of influence. Thus, this method prevents excessive addition of reactive power and control elements to the network, which can make convergence more difficult [8]. For the second category, buses with high voltage instability were measured by the per-unit voltage change at each bus from one N-R iteration to the next. This is given by the equation below:

$$\Delta \dot{V}_{i,k} = \frac{V_{i,k} - V_{i,k-1}}{V_{i,k}} \tag{6}$$

where k is the iteration number; $V_{i,k}$ is the voltage at bus i after iteration k.

These buses have the greatest potential to cause the N-R method to diverge during iterations and they are considered after the ACPF continually diverges for any dispatch adjustment. By default, PSS/E provides information about the bus with the largest $\Delta \dot{V}$ after each iteration.

c) Voltage Tuning at Regulated Buses: After the addition of switched shunt devices at a bus, the algorithm must decide the appropriate voltage schedule (V_{sch}) for the bus. In PSS/E, this is set using voltage bounds (V_{hi} and V_{lo}) centered around the desired V_{sch}. Normally, the choice of these control variables is made by human adjustments using heuristic knowledge until a desired solution is found. However, it is sub-optimal to hard code the algorithm using heuristic knowledge, especially when shunt devices are connected to PQ buses with no initial V_{sch} to reference. Moreover, the initial V_{sch} of some generator buses may require tuning to achieve convergence. Hence, the OPF feature of PSS/E was exploited to allow the algorithm to calculate optimal values for the V_{hi} and V_{lo} of shunt-regulated buses and V_{sch} of generator buses. $\boldsymbol{P}_{\mathrm{gen}}$ of generators are fixed since the desired generators' dispatch are already known, therefore, the implicit objective function of the optimization is given by (7) to tune V_{sch} but also limit its deviation from initial values.

$$f(V_{\mathrm{sch}}) = \rho \sum_{i=1}^{N_{\mathrm{PV}}} \left(V_{\mathrm{sch},i_f} - V_{\mathrm{sch},i_0}\right)^2 \tag{7}$$

where N_{PV} is the number of PV buses; V_{sch,i_f} & V_{sch,i_0} are final and initial values of V_{sch} at bus i; ρ is a scalar quadratic penalty factor.

For generator buses, ρ should be set at a high value to discourage deviation from initial values unless unavoidable. In contrast, ρ should be small for buses regulated with shunt devices to allow free modulation of V_{hi} and V_{lo}. The adjustment of the voltage setpoints is constrained within user-defined limits ($V_{\mathrm{lim,lo}}$ & $V_{\mathrm{lim,hi}}$). PSS/E applies inequality constraints to the optimization problem using a logarithmic barrier function given by (8) [25].

$$B\left(x_{\mathrm{cs}}\right) = - \left(10^{\mu}\right) \sum_{i=1}^{N} \left\{\log\left(x_i - x_{\min,i}\right) + \log\left(x_{\max,i} - x_i\right)\right\} \tag{8}$$

where x_{cs} is a constrained state or control variable; $x_{\min}$ and $x_{\max}$ are the limits of the inequality constraint; μ is a barrier coefficient that regulates closeness of x_{cs} to $x_{\min}$ and $x_{\max}$; N is the number of the x_{cs} variable in the network.

The full optimization problem is therefore defined in (9):

$$L(x, \lambda) = f(x) + B(x) + [\lambda]^{\mathrm{T}}[h(x)] \tag{9}$$

where x is all power system variables (state and control); $f(x)$ is the objective function; $B(x)$ is the barrier function for each inequality constraint; $h(x)$ is the equality constraints including power mismatch equations; λ is the Lagrange multiplier variable.

The standard Kuhn-Tucker criterion is used to formulate the optimality condition and Newton's second-order solution method is adopted to solve the formulated equations [25]. After the optimal voltage setpoints are determined, the ACPF case is solved using the N-R method to ensure the calculated voltage setpoints are stable. At this point, newly added shunt devices with 0 MVAr output are removed.

3) Post-processing

Post-processing is carried out after a solved ACPF solution has been obtained for a target dispatch as follows:

- Q_{gen} of generators at 0 MW output in the target dispatch are converted to shunt devices and these generators are turned off.

- Gradual removal of added MVar compensation.
- Conversion of shunt devices' voltage control from continuous to discrete.

The removal of the added MVar compensation (henceforth called shunt shaving) is performed by the gradual reduction of the capacity of the shunt devices. The ACPF is solved after each reduction until all additional shunt devices are removed or the ACPF stops converging.

The complete flow chart of the hot-starting algorithm is presented in Fig. 4. For the outer loop in Fig. 4 that starts from the "*Check bus voltages*" step, a maximum iteration limit of 200 was set for the algorithm irrespective of the f value.

C. Hardware and Software

The hot-starting incremental algorithm was implemented using the Python 2.7 application platform interface to run the program in PSS/E 34.6.1. A computer with an Intel Core-i7-9700 CPU and RAM of 16.0 GB was used.

III. Case Study: 243-bus Reduced WECC System

The proposed method was evaluated using two sets of hourly generation and load dispatches received from the National Renewable Energy Laboratory (NREL), USA, for the 243-bus reduced WECC system. The reduced system was

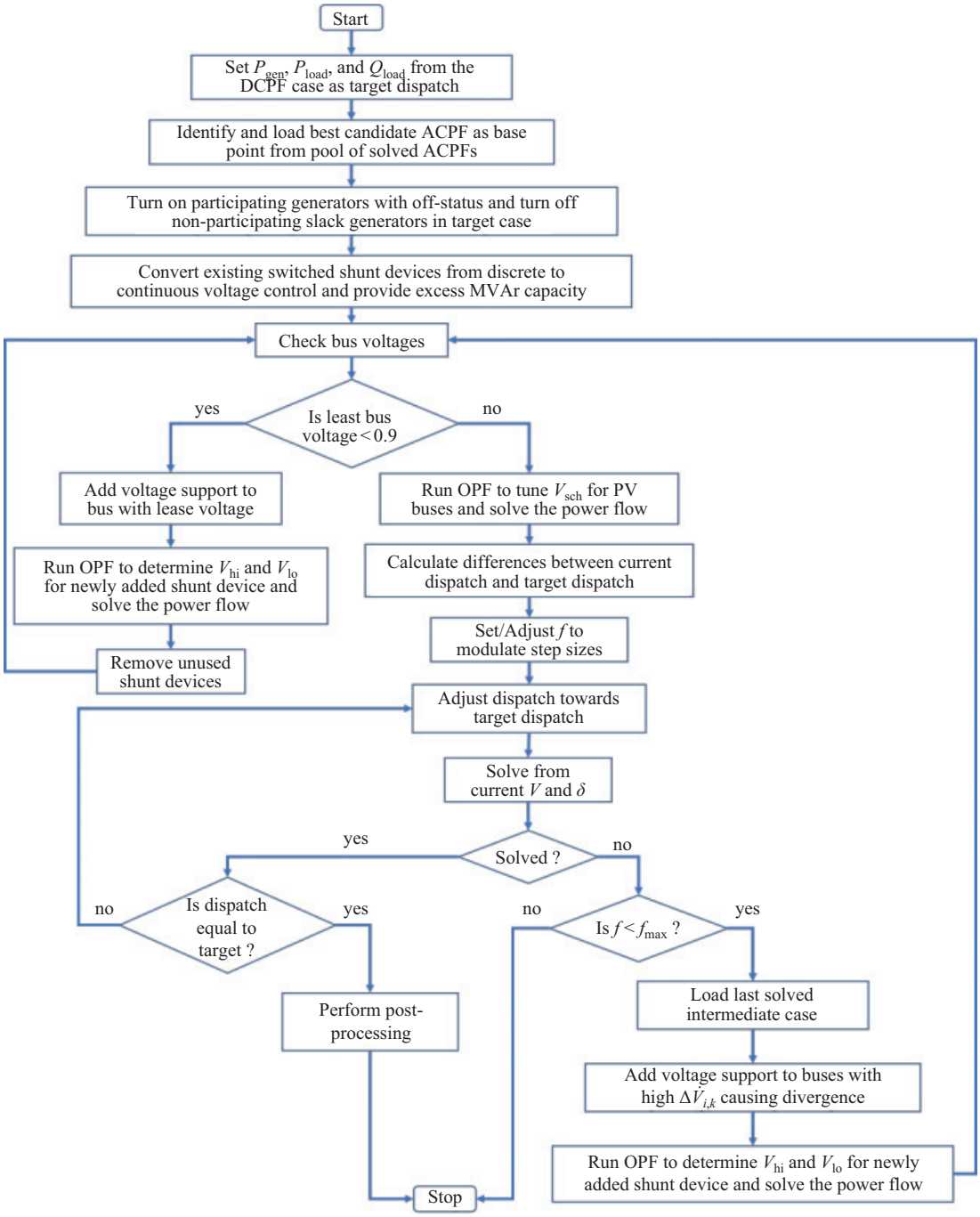

Fig. 4. Flow chart for the hot-starting algorithm.

initially developed in [26], but the generator resource mix has since been updated in [27] as presented in Table I, to better model the actual resource mix in the WECC system. The system has 139 load centers with active and reactive power consumption. The first hourly dispatch set contains 8,784 dispatch cases (*henceforth called Dataset 1*) while the other contains 6,926 dispatch cases (*henceforth called Dataset 2*). Each of these dispatch cases, calculated using DCOPF, only contain $\boldsymbol{P}_{\text{gen}}$, and $\boldsymbol{P}_{\text{load}}$, for several hours in a year. Note that there was no consideration of transmission losses in the DCOPF calculations, these losses would have to be supplied by the slack generators in the corresponding ACPF cases.

TABLE I
GENERATOR RESOURCE MIX IN REDUCED WECC SYSTEM

Generator Type	No. of generator	Max. P capacity (GW)	Max. Q capacity (±GVAr)
Biomass	5	1.8	0.4
Coal	18	44.6	15.4
Diesel	3	0.0	0.0
Gas	47	108.6	35.8
Generic Renewable	1	0.1	0.0
Geothermal	5	4.2	1.4
Hydro	25	60.5	23.4
Nuclear	3	7.7	2.8
Pumped Storage	2	4.3	1.7
Solar	20	28.3	11.0
Wind	17	21.0	5.5

A. Stage 1: The Simple DC-to-ACPF Algorithm

Two separate reference ACPF were obtained for Datasets 1 & 2. These reference ACPF have initial V_{sch} for their regulated buses along with load power factors. Both include existing switched shunt MVar compensators with discrete voltage control on 7 buses with a total capacity of 6,100 MVAr. The simple DC-to-ACPF algorithm in stage 1 was deployed to convert the hourly dispatch cases in both datasets to ACPF. Table II presents the number of ACPF cases in each dataset that were solved at this stage.

TABLE II
CASES SOLVED BY THE SIMPLE DC-TO-ACPF TOOL IN STAGE 1

Dataset	Solved ACPF	Unsolved ACPF
1	8,781	3
2	4,469	2,457

Dataset 2 has many unsolved cases compared to Dataset 1. It was suspected that Dataset 2 may have some errors in its DCOPF calculations, nevertheless, it provided a worst-case scenario for the evaluation of the hot-starting algorithm. Table III shows the percentage of the solved cases with at least one bus violating various voltage limits and the average number of buses at which the violations occur.

Note the initial V_{sch} in both reference ACPF range from 1.0 to 1.128 p.u., thus the acceptable voltage range across the network was taken to be 0.9 to 1.14 p.u. Table III shows the proportion of solved cases in Dataset 2 that have violating buses is greater than in Dataset 1, but only a few buses per violating case exceed the voltage limits.

B. Stage 2: The Hot-starting Incremental Algorithm

The unsolved cases from stage 1 were passed to stage 2 where the developed hot-starting algorithm was used to solve them. For Dataset 1 with three unsolved cases, their dispatches (P_{gen}, P_{load} & Q_{load}) were set as target dispatch. Then the algorithm found the most suitable starting base cases from the pool of already-solved cases in stage 1 as shown in Table IV. The cases are represented as m-d-h, where m, d, and h, are month, day and hour of dispatch respectively. The search for the most suitable starting base case was restricted to solved cases in the same month as the target dispatch to increase search speed. Thus, the average search time was about 4.4 s. Table IV shows the most suitable starting base case for Case 1 is on a different day, 122 hours away. This justifies the deployment of the proposed search method over choosing the nearest solved case. Moreover, some datasets may not be delineated as hours in a year, making it impossible to know the nearest solved case in time.

To run the hot-starting incremental algorithm, certain user-defined variables are required as explained in Section III.B.2. For this case study, the values used for these variables are shown in Table V.

The properties of the final ACPF cases created by the hot-starting algorithm with respect to the target dispatches are presented in Table VI. $\Delta P_{\text{gen,ave}}$, $\Delta P_{\text{gen,max}}$, $\Delta P_{\text{load,ave}}$, and $\Delta P_{\text{load,max}}$, are all zero, showing the algorithm successfully adjusted the generator and load dispatch of the starting base cases to the same values as the target dispatch. Therefore, it indirectly solved the ACPF-equivalent of the target dispatch case. The table also shows significant differences between MVar compensation from the shunt devices before and after shunt shaving. This capability of the hot-starting algorithm to add appropriate voltage support for ACPF solution will be useful to power systems planners to reveal reactive power requirements of a grid under future dispatch scenarios. Fig. 5 shows the $\boldsymbol{V}_{\text{sch}}$ of the generators in the three cases compared to the initial $\boldsymbol{V}_{\text{sch}}$ in the reference cases. To obtain a solution, the hot-starting algorithm was able to automatically tune the $\boldsymbol{V}_{\text{sch}}$ with limited deviation from the initial $\boldsymbol{V}_{\text{sch}}$ and within the defined voltage limits in Table V. Furthermore, Fig. 5 shows

TABLE III
PROPORTION OF SOLVED CASES VIOLATING VOLTAGE LIMITS IN STAGE 1

Voltage ranges (p.u.)	Dataset 1		Dataset 2	
	% of solved cases with violations	Average no. of violating buses per violating case	% of solved cases with violations	Average no. of violating buses per violating case
< 0.90 or > 1.14	43.8%	1.27	61.60%	2.04
< 0.85 or > 1.17	0.28%	2.50	16.65%	1.40
< 0.80 or > 1.20	0.046%	5.75	3.18%	1.19

TABLE IV
STARTING BASE CASES TO HOT-START ACPF SOLUTION

Case	Target dispatch	Starting base case
1	10–31–16	10–26–13
2	10–8–21	10–8–22
3	12–8–19	12–8–20

TABLE V
USER-DEFINED VARIABLES FOR HOT-STARTING ALGORITHM

User-defined variables	Case study values
f_{init}	0.05
Δf	0.3 $\times f$
$f_{\max}$	2
ρ	10,000
$V_{\text{lim,lo}}$	0.9
$V_{\text{lim,hi}}$	1.14
μ	0.0001

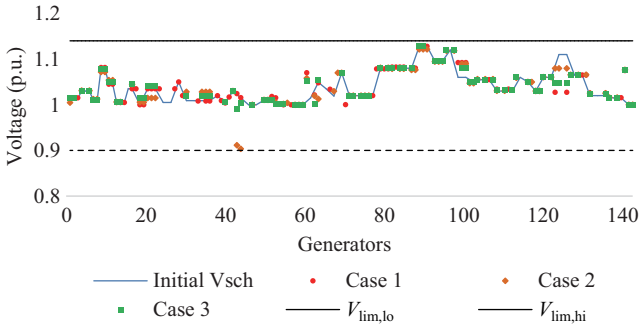

Fig. 5. Initial V_{sch} and tuned V_{sch} for the final ACPF of the 3 cases.

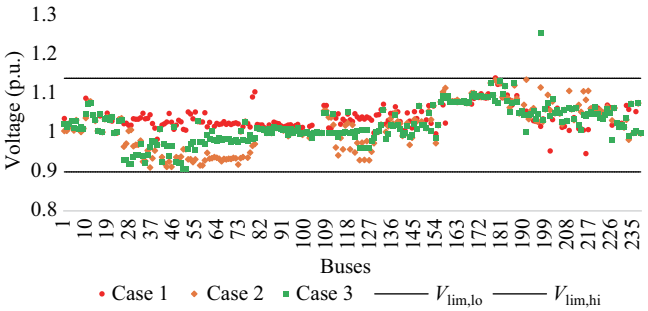

Fig. 6. Bus Voltages for the final ACPF of the 3 cases.

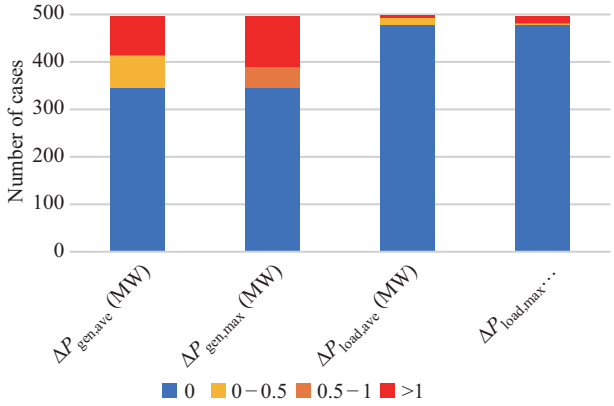

Fig. 7. Differences between target dispatch and dispatch in the ACPF cases solved by the hot-starting algorithm.

that only one bus in Case 3 violates the prescribed upper voltage limit, all other buses in the three cases have voltages within the set limits. This shows the ability of the hot-starting algorithm to provide ACPF solutions with desirable voltage levels at a target dispatch.

For Dataset 2 with suspect dispatches, 500 random cases were selected out of the unsolved cases. $V_{\text{lim,hi}}$ and $V_{\text{lim,lo}}$ were ignored to allow for convergence since about two-thirds of the solved cases in stage 1 have buses that violate voltage limits (see Table III). All other parameters in Table V were kept constant. The algorithm reached the maximum iteration limit for 6 out of the 500 cases, so results for these were not presented. $\Delta P_{\text{gen,ave}}$ and $\Delta P_{\text{gen,max}}$ plotted on Fig. 6 show that the ACPF created for 345 dispatch cases reached their target dispatch with zero deviation. 44 more ACPF cases had dispatches close to their target dispatches with $\Delta P_{\text{gen,ave}}$ and $\Delta P_{\text{gen,max}}$ in the range of 0–0.5 MW and 0.5–1 MW respectively. If this is set as a success criterion (i.e., $\Delta P_{\text{gen,ave}} \leq 0.5$ MW and $\Delta P_{\text{gen,max}} \leq 1$ MW), then the success rate of the hot-starting algorithm is 77.8% for the cases in Dataset 2.

Figure 8 is a plot of the number and capacity of retained shunt devices after shunt shaving for the ACPF cases that passed the success criterion. Many of these cases require significant MVar compensation to maintain ACPF convergence. This shows the operating conditions of these cases were not within their RS. Thus, it was necessary for the algorithm to add and retain MVar compensation to increase RS and avoid compromising the ACPF solutions. Finally, Fig. 9 shows the run time of the algorithm can be highly disparate, ranging from some seconds to several minutes. The average run times for cases that passed and failed the success criterion were 34.2 s

TABLE VI
PROPERTIES OF THE ACPF CREATED BY THE HOT-STARTING ALGORITHM WITH RESPECT TO TARGET DISPATCH

Properties	Case 1		Case 2		Case 3	
	Starting Base case ACPF	Final ACPF	Starting Base case ACPF	Final ACPF	Starting Base case ACPF	Final ACPF
Average $\boldsymbol{P}_{\text{gen}}$ difference w.r.t target dispatch, $\Delta P_{\text{gen,ave}}$ (MW)[a]	312.30	0.0	88.05	0.0	50.87	0.0
Maximum $\boldsymbol{P}_{\text{gen}}$ difference w.r.t target dispatch, $\Delta P_{\text{gen,max}}$ (MW)[a]	3310.64	0.0	1449.40	0.0	1449.40	0.0
Average $\boldsymbol{P}_{\text{load}}$ difference w.r.t target dispatch, $\Delta P_{\text{load,ave}}$ (MW)	50.65	0.0	31.74	0.0	10.02	0.0
Maximum $\boldsymbol{P}_{\text{load}}$ difference w.r.t target dispatch, $\Delta P_{\text{load,max}}$ (MW)	370.49	0.0	248.40	0.0	63.00	0.0
Q from switched shunt devices before shunt shaving [No. of devices] (MVAr)	3097.27 [15]		3582.55 [34]		4082.15 [31]	
Q from switched shunt devices after shunt shaving [No. of devices] (MVAr)	1198.47 [2]		776.99 [5]		261.73 [3]	
Algorithm run time (s)	24.7		20.2		21.9	

[a]Excluding slack generator

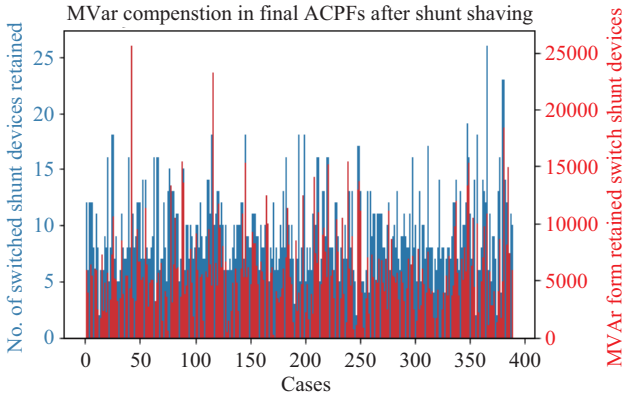

Fig. 8. MVar compensation in the solved ACPF cases that passed the success criterion in Dataset 2.

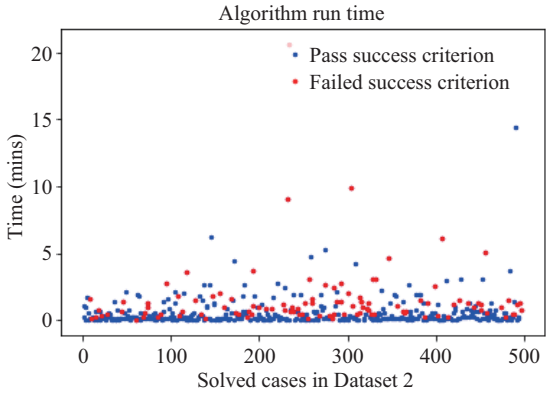

Fig. 9. Algorithm run time for the solved ACPF cases in Dataset 2.

and 92.1 s respectively, while the overall average run time is 46.7 s.

IV. Conclusion

This work explores the use of a two-stage approach to convert dispatch cases from DCOPF to ACPF with minimal human intervention. The first stage attempts to solve the formulated ACPF cases using N-R method from the generic flat start. Unsolved cases in the first stage are passed down to the second stage where a hot-starting incremental algorithm indirectly solves their ACPF from a suitable base case while automatically adding MVar compensation and tuning voltage setpoints. Conversion of two sets of dispatch cases was used as a case study to test the performance of the proposed conversion method. The first dataset represented a typical scenario with reasonably accurate dispatch cases while the other represented an extreme scenario with suspect dispatch cases. The algorithm based on the proposed methods successfully converted 100% of the dispatch cases in the first dataset to solved ACPF and 77.8% were converted in the second dataset. It was noted that algorithm run time is highly disparate ranging from some seconds to several minutes, the average run time for about 500 solved cases was less than 1 minute. Sub-methods of the deployed hot-starting algorithm such as the OPF-based tuning of voltage setpoints and automated MVar compensation addition can be used to replace heuristics in choosing generators voltage schedule and reactive power planning respectively.

Future work will focus on using the proposed method for larger power systems such as the full WECC model with 10,000 buses. The voltage setpoint tuning method may require some modifications since the optimization technique deployed can be slow for some large systems. It will also be desirable to develop automatable methods to identify inaccurate dispatches from DCOPF before conversion to ACPF commences.

Acknowledgment

The authors acknowledge Dr. Jin Tan and Dr. Haoyu Yuan from National Renewable Energy Laboratory, and Dr. Jianhui Wang and Dr. Yanling Lin from Southern Methodist University for providing the hourly dispatch data used in this study. The data was created in the work sponsored by the U.S. Department of Energy Solar Energy Technologies Office under Award #34224.

References

[1] A. S. Ahmadyar, S. Riaz, G. Verbič, A. Chapman, and D. J. Hill. (2017, Aug.). A framework for frequency stability assessment of future power systems: an australian case study. [Online]. Available: https://arxiv.org/pdf/1708.00739.pdf

[2] R. D. Liu, G. Verbič, J. Ma, and D. J. Hill, "Fast stability scanning for future grid scenario analysis," *IEEE Transactions on Power Systems*, vol. 33, no. 1, pp. 514–524, Jan. 2018.

[3] M. B. Cain, R. P. O'Neill, and A. Castillo. (2012, Dec.). History of optimal power flow and formulations - optimal power flow paper 1. Federal Energy Regulatory Commission. [Online]. Available: https://www.ferc.gov/sites/default/files/2020--05/acopf-1-history-formulation-testing.pdf

[4] X. F. Wang, Y. H. Song, and M. Irving, *Modern Power Systems Analysis*, New York: Springer, 2008.

[5] T. J. Overbye, "A power flow measure for unsolvable cases," *IEEE Transactions on Power Systems*, vol. 9, no. 3, pp. 1359–1365, Aug. 1994.

[6] A. Klos and A. Kerner, "The non-uniqueness of the load flow solution," in *Proceedings of the 5th Power Systems Computing Conference* (*PSCC*), Cambridge, 1975.

[7] M. L. Crow, *Computational Methods for Electric Power Systems*, Boca Raton: CRC Press, 2010.

[8] T. J. Overbye, X. Cheng, and Y. Sun, "A comparison of the AC and DC power flow models for LMP calculations," in *Proceedings of the 37th Annual Hawaii International Conference on System Sciences*, 2004.

[9] National Academies of Sciences, Engineering, and Medicine, *Analytic Research Foundations for the Next-Generation Electric Grid*, Washington: The National Academies Press, 2016.

[10] B. Stott, "Effective starting process for Newton-Raphson load flows," *Proceedings of the Institution of Electrical Engineers*, vol. 118, no. 8, pp. 983–987, Aug. 1971.

[11] G. Leoniopoulos, "Efficient starting point of load-flow equations," *International Journal of Electrical Power & Energy Systems*, vol. 16, no. 6, pp. 419–422, Dec. 1994.

[12] B. Stott, J. Jardim, and O. Alsac, "DC power flow revisited," *IEEE Transactions on Power Systems*, vol. 24, no. 3, pp. 1290–1300, Aug. 2009, doi: 10.1109/tpwrs.2009.2021235.

[13] H. H. Müller, M. J. Rider, and C. A. Castro, "Artificial neural networks for load flow and external equivalents studies," *Electric Power Systems Research*, vol. 80, no. 9, pp. 1033–1041, Sep. 2010.

[14] L. J. Chen and J. E. Tate. (2020, Apr.). Hot-starting the ac power flow with convolutional neural networks. [Online]. Available: https://arxiv.org/pdf/2004.09342.pdf

[15] B. Vyakaranam, K. Mahapatra, X. Y. Li, H. Wang, P. Etingov, Z. S. Hou, Q. Nguyen, T. Nguyen, N. Samaan, M. Elizondo, and T. Hay, "Novel data-driven distributed learning framework for solving AC power flow for large interconnected systems," *IEEE Open Access Journal of Power and Energy*, vol. 8, pp. 281–292, Jun. 2021, doi: 10.1109/oajpe.2021.3092264.

[16] S. Cvijic, P. Feldmann, and M. Hie, "Applications of homotopy for solving AC power flow and AC optimal power flow," in *Proceedings of 2012 IEEE Power and Energy Society General Meeting*, San Diego, USA, 2012, pp. 1–8.

[17] W. Murray, T. T. De Rubira, and A. Wigington, "Improving the robustness of Newton-based power flow methods to cope with poor initial points," in *Proceedings of 2013 North American Power Symposium* (*NAPS*), Manhattan, USA, 2013, pp. 1–6.
[18] S. Granville, J. C. O. Mello, and A. C. G. Melo, "Application of interior point methods to power flow unsolvability," *IEEE Transactions on Power Systems*, vol. 11, no. 2, pp. 1096–1103, May 1996.
[19] Z. Feng, V. Ajjarapu, and D. J. Maratukulam, "A practical minimum load shedding strategy to mitigate voltage collapse," *IEEE Transactions on Power Systems*, vol. 13, no. 4, pp. 1285–1290, Nov. 1998.
[20] L. V. Barboza and R. Salgado, "Corrective solutions of steady state power system via newton optimization method," *SBA Controls & Automation*, vol. 11, no. 3, pp. 182–186, Sep. 2000.
[21] B. Vyakaranam, Q. H. Nguyen, T. B. Nguyen, N. A. Samaan, and R. Huang, "Automated tool to create chronological AC power flow cases for large interconnected systems," *IEEE Open Access Journal of Power and Energy*, vol. 8, pp. 166–174, Apr. 2021, doi: 10.1109/oajpe.2021.3075659.
[22] S. Seo, S. G. Kang, B. Lee, T. K. Kim, and H. Song, "Determination of reactive power compensation considering largedisturbances for power flow solvability in the Korean power system," *Journal of Electrical Engineering and Technology*, vol. 6, no. 2, pp. 147–153, Mar. 2011.
[23] H. N. Dinh, M. Y. Nguyen, and Y. T. Yoon, "A new approach for corrective and preventive control to unsolvable case in power networks having DERs," *Journal of Electrical Engineering and Technology*, vol. 8, no. 3, pp. 411–420, May 2013.
[24] A. B. Birchfield, T. Xu, and T. J. Overbye, "Power flow convergence and reactive power planning in the creation of large synthetic grids," *IEEE Transactions on Power Systems*, vol. 33, no. 6, pp. 6667–6674, Nov. 2018.
[25] *PSS/E 34.6.1 Program Operation Manual*, New York: Siemens Industry, Inc., 2019.
[26] J. E. Price and J. Goodin, "Reduced network modeling of WECC as a market design prototype," in *Proceedings of 2011 IEEE Power and Energy Society General Meeting*, 2011, pp. 1–6.
[27] H. Y. Yuan, R. S. Biswas, J. Tan, and Y. C. Zhang, "Developing a reduced 240-bus WECC dynamic model for frequency response study of high renewable integration," in *Proceedings of 2020 IEEE/PES Transmission and Distribution Conference and Exposition*, Chicago, USA, 2020.

Adedasola A. Ademola (Student Member, IEEE) received a B.S. in Electrical & Electronic Engineering from University of Ibadan, Nigeria, in 2016. He received his M.S. in Sustainable Energy Systems from University of Edinburgh, UK, in 2018. He is currently pursuing an interdisciplinary Ph.D. degree at the University of Tennessee, Knoxville, TN, USA. His research interests include power flow studies under extreme conditions, renewable energy integration, and artificial intelligence.

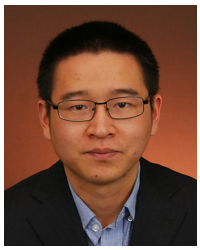

Shutang You (Member, IEEE) received a B.S. and M.S. degrees in Electrical Engineering from Xi'an Jiaotong University in 2011 and 2014, respectively, and a Ph.D. degree in Electrical Engineering from the University of Tennessee, Knoxville, in 2017, where he is currently a Research Assistant Professor with the Department of Electrical Engineering and Computer Science. His research interest is in power grid dynamics and monitoring.

Yilu Liu (F'04) received a M.S. and Ph.D. degrees from The Ohio State University, Columbus, OH, USA, in 1986 and 1989, respectively. She was a Professor with Virginia Tech. She led the effort to create the North American power grid Frequency Monitoring Network at Virginia Tech, which is currently operated at The University of Tennessee, Knoxville, (UTK), TN, USA, and the Oak Ridge National Laboratory (ORNL) as GridEye. She is currently the Governor's Chair with UTK and ORNL. Her current research interests include power system wide-area monitoring and control, large interconnection level dynamic simulations, electromagnetic transient analysis, and power transformer modeling and diagnosis. She is a member of the U.S. National Academy of Engineering.